# Wound Healing: Multi-Scale Modeling

**Fred J. Vermolen and Amit Gefen**

**Abstract** This chapter is meant as an overview of our already published work that we carry out on modeling wound healing on the cellular, colony and tissue scale, though we detail the description of some stochastic principles that appear in our models. The relation between the scales is described in terms of the underlying biological and mathematical concepts. We also present the implications and applicability of the mathematical models studied.

## 1 Introduction

Wound healing is a very complicated process with the following partly overlapping phases: inflammation—proliferation—remodeling. During the post-bleeding inflammatory phase macrophages and white blood cells (leukocytes) enter the wound site to clear up invading harmful agents and bacteria through the broken network of capillaries. If a patient suffers from diabetes, then the capillary walls are suffering from an increased stiffness by which they can break down, and extend less due to a decreased flexibility, and thereby transport less blood containing oxygen and indispensable nutrients. Co-agulation of blood occurs to shut-off the wound. This is followed by angiogenesis, to restore the capillary network, dermal regeneration, which involves contraction due to traction forces exerted by

F. J. Vermolen (✉)
Delft Institute of Applied Mathematics, Delft University of Technology,
Mekelweg 4, 2628 Delft, The Netherlands
e-mail: f.j.vermolen@tudelft.nl

A. Gefen
Department of Biomedical Engineering, Tel Aviv University, Tel Aviv, Israel
e-mail: gefen@eng.tau.ac.il

Stud Mechanobiol Tissue Eng Biomater (2013) 14: 321–345
DOI: 10.1007/8415_2012_156

Published Online: 25 November 2012

(myo-)fibroblasts, as well as wound closure by the keratinocytes that form the basis of the epidermis (epithelium).

Many in-vitro experimental and clinical in-vivo studies have been carried out to scrutinize the biological mechanisms that take place during the very complex process of wound healing. Unfortunately, still many of the underlying biology is still unclear despite the long lasting research in wound healing. In order to improve and to prevent wounds, such as pressure ulcers or diabetic ulcers, it is important to quantify the influence of the related partial processes taking place during the healing of wounds. This quantification can be done using statistical analyses on raw data using for instance genetic algorithms or other forms of artificial intelligence such as neural networks. Since much data lack detailed quantitative aspects, this holds for in-vivo data in particular, mathematical modeling is also a very helpful tool for the quest of the interrelations between the parameters involved. The challenge is either to build a complicated mathematical model that contains as many of the biological parameters as possible, or to construct simple models that contain a minimum number of parameters such that only those parameters and processes that have the largest impact on the healing kinetics are taken into account. The first class of models will involve many biological parameters that need to be determined using complicated inverse modeling or any other type of regression analysis, in which the valid question arises whether the set of parameters determined is the actual solution or that one should take another combination of the parameters involved which reproduces the experiments (almost) equally well. In other words, the question of uniqueness arises in a natural setting. This concern is overcome by the construction of a simplified formalism of a certain (partial) biological process occurring in wound healing. In this paper, we will highlight the latter class of mathematical models: simplified models for partial processes occurring during wound healing. We will look at models designed for various scales and attempt to describe the relations between these models in terms of the underlying biology and mathematics.

Since wound healing involves basic biological processes like cell migration as a result of chemico-mechanical stimuli and random walk, cell proliferation and growth, cell differentiation, cell death, secretion and signaling of growth factors, we will incorporate many of these processes in a different way into the models at the various scales considered. To apply these processes, one basically considers the following mathematical approaches:

- Continuum-based partial differential equations involving transport (random walk, chemo-tenso taxis) and mechanical balances (visco-elasticity) on a tissue scale;
- Cellular scale involving discrete lattice models like the cellular Potts model, cellular automata models (involving a minimization of a virtual energy with a Monte-Carlo like scheme), or the continuous semi-stochastic approach by Vermolen and Gefen [1] and Byrne and Drasdo [2];

- Phenomenological models where the wound healing is modeled as a moving boundary problem where the interface moves as a result of a growth factor and local curvature.

The first approach involves very complicated models where many badly known biological input-parameters are needed. A big advantage is the fact that these models take relatively many biological parameters and subprocesses into account and that large tissue areas and large wounds can be modeled. This class of models can be applied to real-like in-vivo wounds of the order of centimeters or even larger. The domain of computation needs to be discretized to obtain a finite-element (or any other discretization) discretization in order to approximate the solution of the resulting boundary value problems formulated in terms of partial differential equations and its initial/boundary conditions. The parameter space and limited availability of appropriate values is a serious drawback of this class of models. An example concerns the availability of diffusion coefficients (i.e. random walk) or chemotactic coefficients or proliferation coefficients, see [3–6, 7–10, 11, 12, 13, 14, 15, 16] to mention a few of them. The second class of models only takes few parameters into account, but stays close to biology if one models in-vitro experiments. An extension to in-vivo cases is not straightforward since one typically will need to consider a large domain of computation and thereby making the number of cells or lattice points to be considered extraordinarily large. However, information from experiments concerning cell motility as a function of the acidity for instance, can be incorporated in a relatively straightforward manner. Examples are the studies presented in [1, 2, 17, 18, 19, 20]. The third model class takes few parameters as well, however, there is not much biology involved. An advantage of this class of models is, if the model has been set up in a clever way, that the small number of parameters involved can be adjusted such that experimental cases can be modeled in both in-vitro and in-vivo situations. See for the instance [21, 9, 22, 23].

In the manuscript, we will describe these classes of models and discuss their applicability. We will mainly focus on a recently developed continuity-based model from the second class on cellular level. Of course the models from the cellular automata-class, such as the cellular Potts model, can be positioned in the same kind of models. This continuous-based model mimics the migration of a collection of cells on a planar substrate, where we also take into account a bacterially infected zone where an increased acidity, resulting from the competition of cells and bacteria on oxygen and nutrients, impairs cellular mobility without the use of a predefined computational lattice. We will show some examples of simulations. In this model cell motion is a partly stochastic process. Cell death and cell division are modeled as stochastic processes. The original formulation of the model can be found in Vermolen and Gefen [1]. Furthermore, we will show some results from a newly constructed cell deformation model under the influence of chemotaxis. Finally, we address how the results from a small scale model can be used as input for a large scale model.

## 2 Mathematical Models: From Cell Scale to Tissue Scale

In this section, we consider some mathematical models at various scales where we introduce the models first to make the present manuscript complete. In the next chapter, we will describe the link between modeling at various scales in terms of the underlying biology and mathematics. In this chapter, we will mainly focus on cell migration, proliferation and death.

### *2.1 The Cell Scale*

In this class of model, we consider the deformation during migration of individual cells. The cells are assumed to migrate as a result of a chemical signal. We bear in mind that the mathematical description of the influencing signal is generic and can easily be adapted and used to model cell deformation and growth as a result of a mechanical signal.

#### 2.1.1 Random Walk: From Bacteria or Cells to Probability

The model can be applied to bacterial sources where individual bacteria make the surrounding tissue more acid by the effective production of biotic lactates as a result of the competition between the bacteria and cells for the available nutrients and oxygen, which make white blood cells move towards the infectious bacteria, or it can be applied, for instance, to the migration of fibroblasts or keratinocytes, among others, towards the wound region due to the signaling agents released by platelets that are in the coagulated area of the wound. In the case of modeling individual randomly moving bacteria, we use a random walk model with a stochastic differential equation based on Ito-processes. The model may also incorporate the bacteria in an upscaled way so that only bacterial densities are considered. First, we consider the individual random walk of bacteria. Then, in three dimensions, the equation of motion does not contain any deterministic drift, hence for the motion of the bacterium, we obtain

$$dX(t) = \sigma dW(t), \qquad dY(t) = \sigma dW(t), \qquad dZ(t) = \sigma dW(t), \qquad \text{for } t > 0, \tag{1}$$

subject to the prescribed initial bacterial condition $(X(0), Y(0), Z(0)) = (X_0, Y_0, Z_0)$, where the co-ordinate positions are independent. Here $W(t)$ is a Wiener process, or Brownian Motion such that the position of the bacterium is distributed normally with mean coordinates $(X_0, Y_0, Z_0)$ and variance of $\sigma^2 t$ for each coordinate direction. Formally, the Wiener process satisfies the following requirements:

- $W(0) = 0$;
- The increments, $W(t_{k+1}) - W(t_k)$ and $W(t_k) - W(t_{k-1})$ are independent for any $0 \leq t_{k-1} < t_k < t_{k+1}$;
- For $0 \leq s \leq t$, the increment $W(t) - W(s)$ has the Gaussian distribution with mean 0 and variance $t - s$, i.e. $W(t) - W(s) \sim N(0, t - s)$.

Further, $W(t)$ is 'stochastically continuous' ($\lim_{t \to s} P(|W(t) - W(s)| > \epsilon) = 0$), where $P$ stands for the probability. The formal analytic solution,

$$X(t) = X_0 + \sigma W(t), \qquad Y(t) = Y_0 + \sigma W(t), \qquad Z(t) = Z_0 + \sigma W(t), \quad \text{for } t > 0, \tag{2}$$

can be given, however the differential form is more useful in this study from a practical point of view. The equations are classically numerically solved using the Euler–Maruyama Method, given by

$$\hat{\mathbf{X}}_{i+1} = \hat{\mathbf{X}}_i + \sigma \Delta \mathbf{W}_{i+1}, \qquad \hat{\mathbf{X}}_0 = (X_0, Y_0, Z_0). \tag{3}$$

Here each component of $\Delta \mathbf{W}$ is a normally distributed stochastic parameter with zero mean and variance $\Delta t$, denoted by $N(0, \Delta t)$, and it can be proved that [24] each component $v$ satisfies $\Delta W^v_{i+1} = W^v_{i+1} - W^v_i \sim N(0,1)\sqrt{\Delta t}$, in other words, a Gaussian distribution with zero mean and a variance of $\Delta t$. We show a run of the solution of the stochastic differential equations with one bacterium initially located at $(0, 0, 0)$ with mobility $\sigma = 2.6833 \cdot 10^{-5}$ m/$\sqrt{s}$. This value was chosen from [25] and corresponds to the classical bacillum in Fig. 1. Figure 1 shows the trajectory of the bacterium over time in three dimensions. Since Fig. 1 only gives one specific run, the trajectory itself is a stochastic parameter and hence for many purposes the probability density function is of more importance. To this extent, since $dW(t) \sim N(0,1)\sqrt{dt}$ and $W(t) \sim N(0,1)\sqrt{t}$, the probability density for the position of the bacterium at time $t$ for each coordinate direction satisfies

$$f_v(t, v) = \frac{1}{\sqrt{2\pi\sigma^2 t}} \exp\left(-\frac{(v - v_0)^2}{2\sigma^2 t}\right), \qquad v \in (X, Y, Z). \tag{4}$$

Since the Brownian motion in each coordinate direction is an independent stochastic event, the multi-variate probability density is given by

$$f(x, y, z) = \frac{1}{(2\pi\sigma^2 t)^{\frac{3}{2}}} \exp\left(-\frac{(\mathbf{x} - \mathbf{X}_0)^2}{2\sigma^2 t}\right), \tag{5}$$

which solves the initial value problem in $\mathbb{R}^3$

$$\frac{\partial f}{\partial t} - \frac{\sigma^2}{2} \Delta f = 0, \qquad f(0, (x, y, z)) = \delta(\mathbf{x} - \mathbf{X}_0). \tag{6}$$

Here $\delta(\mathbf{x})$ represents the Dirac Delta Distribution in three dimensions, with characteristics

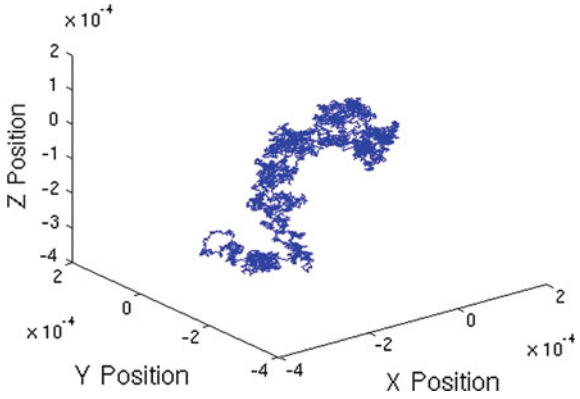


**Fig. 1** The trajectory of a bacterium originally located at $(0,0,0)$ and moving according to Brownian motion with $\sigma = 2.6833 \cdot 10^{-5}$ m/$\sqrt{\text{s}}$, which corresponds to a bacillum at 37 °C

$$\begin{aligned} &\delta(\mathbf{x}) = 0, \text{ for all } (x,y,z) \neq (0,0,0), \\ &\int\limits_{\Omega \ni (0,0,0)} \delta(x,y,z) d\Omega = 1, \end{aligned} \tag{7}$$

where $\Omega$ is subset of $\mathbb{R}^3$ with nonzero measure. For $\frac{\sigma^2}{2}$, which represents the diffusivity, we used $\frac{\sigma^2}{2} = 3.6 \cdot 10^{-10}$ m$^2$/s (bacillum at 37 °C). Note that if $D$ represents the diffusivity of a species, then $\sigma = \sqrt{2D}$. Equation (5) represents a fundamental solution to the three-dimensional diffusion equation (in an unbounded domain), and it represents the probability density that the bacterium is localized at position $(x,y,z)$ at time $t$. Note that Eq. (5) is very helpful in deriving the relation between the stochastic differential equation of Langevin type with zero drift, see Eq. (1) and the diffusion equation (12). The probability that a region $\Omega$ contains the bacterium at time $t$ is then given by

$$P(t,\Omega) = \int\limits_{\Omega} f(t,(x,y,z)) d\Omega, \tag{8}$$

and note that $\int_{\mathbb{R}^3} f(t,(x,y,z)) d\Omega = 1$ for $t \geq 0$. We remark that if drift is incorporated through $\mu = (\mu_x, \mu_y, \mu_z)$, then Eq. (1) becomes

$$dX(t) = \mu_x dt + \sigma dW(t), \quad dY(t) = \mu_y dt + \sigma dW(t), \quad dZ(t) = \mu_z dt + \sigma dW(t), \tag{9}$$

for $t > 0$, with exact solution, if $\mu_x, \mu_y, \mu_z$ and $\sigma$ are constant,

$$\begin{aligned} X(t) &= X_0 + \mu_x t + \sigma W(t), \quad Y(t) = Y_0 + \mu_y t + \sigma W(t), \\ Z(t) &= Z_0 + \mu_z t + \sigma W(t), \end{aligned} \tag{10}$$

It is easy to check the validity of the exact solution using Ito's calculus. The drift term could possibly result from chemotaxis or fluid flow and induces a temporarily shifting mean in the probability density, hence Eq. (5) is altered into

$$f(x,y,z) = \frac{1}{(2\pi\sigma^2 t)^{\frac{3}{2}}} \exp\left(-\frac{(\mathbf{x}-\mu t)^2}{2\sigma^2 t}\right). \tag{11}$$

It can be shown by the use of some elementary algebra that this function solves the Fokker–Planck equation

$$\frac{\partial f}{\partial t} + \nabla \cdot (\mu f) - \frac{\sigma^2}{2}\Delta f = 0, \qquad f(0,(x,y,z)) = \delta(\mathbf{x}-\mathbf{X}_0). \tag{12}$$

The above concepts are very standard and were, for the case of unbiased random walk, originally derived by Einstein to study Brownian motion of a particle. Note that we modeled the bacteria as point-sources so far. The extension to multiple bacteria, say $n$, is somewhat straightforward upon approximating the bacterial motion of each bacterium as independent stochastic processes. The probability follows from the binomial distribution that is used to compute the probability of $k$ successes out of $n$ trials where the probability of success is given by $p$. Since then the probability that a certain region, say $\Omega$ possesses $k \leq n$ bacteria is determined through

$$p(t,\Omega;k) = \binom{n}{k} (P(t,\Omega))^k (1-P(t,\Omega))^{n-k}. \tag{13}$$

Hence the probability that this region $\Omega$ contains at least one bacteria is given by

$$p(t,\Omega;k \geq 1) = 1 - (1-P(t,\Omega))^n \approx nP(t,\Omega), \tag{14}$$

where the last approximation is only accurate for $P(t,\Omega) \ll 1$. This approximation enables us to approximate the probability density function for $n$ particles by $nf(t,(x,y,z))$ at those positions away from the initial bacterial positions. Note also that for $t > 0$ the probability density function(s) becomes finite at each position and that we can take the limit $\text{meas}(\Omega) \to 0$, to get an arbitrarily small probability as the volume considered tends to zero. Hence the approach can be extended to solving $f$ in the case of a multi-bacterial environment under the application of the superposition principle for linear diffusion equations. These concepts can be used to model the bacterial density using the same partial differential equations. One can also evaluate a convolution over the domain of computation to get the bacterial density in case of a (piecewise) continuous initial bacterial distribution.

### 2.1.2 A Cell Deformation Model

In the literature, many models for cell deformation exist [26, 17], to mention a few of them. As far as we know, one of the major issues is that most of these models

are based on the solution of partial differential equations, and often the level-set method is used to compute the position of the cell boundary, see for instance [26]. The level-set method requires the solution of a set of partial differential equations, such as the level-set function itself, whose zero level curve typically coincides with the cell boundary, the extension of the boundary velocity and a tedious re-initialization procedure which can be done by the fast-marching method based on the shortest-path optimization procedure, or via the solution of another nonlinear partial differential equation. Despite the enormous flexibility of the level-set method in terms of the ability to track interfaces also in cases where topological changes take place, the method is very expensive. Therefore, we choose to present a simpler method, which has been published only very recently in Vermolen and Gefen [17]. This model is based on the sensitivity of cells to a chemical and can therefore be applied to simulate cell migration and deformation as a result of chemotaxis. To this extent, the cell boundary, either in 2D or in 3D, is divided into gridnodes, which have the ability to move according to the gradient of the concentration of a certain chemical. This chemical could be a source of nutrition, oxygen, a growth factor or a poisonous chemical. Further, these points are connected to their neighbors and to the nucleus via springs, see Fig. 2 for a schematic representation. In this way, surface tension of the cell membrane and the connection between the membrane and nucleus via the ligaments in the cytoplasm are dealt with. First, we consider the modeling of the chemical sources and subsequently we consider the equations of motion of the points on the cell boundary.

To approximate the concentration of the chemical that gives raise to chemotaxis, we will use an approach based on Fundamental solutions of the diffusion equations in unbounded domains such as Eq. (5). For the release of the chemical

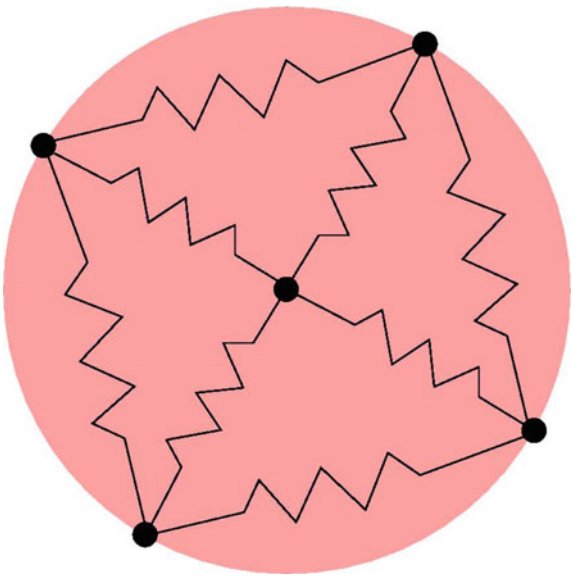

**Fig. 2** A schematic of the distribution of springs that forms the backbone of the cell skeleton in the model

agent that attracts cells, we assume all sources to be very small compared to cell areas and therefore, we approximate these sources as *point-sources*. Here, we will assume that a point source is able to move, for instance via Brownian motion, but that the diffusion-field that surrounds it, sets in either instantaneously or gradually builds up in time. These point sources can correspond to either bacteria or to points on the cell boundary of other cells. First we consider the *instantaneous* diffusion field. For this purpose, we consider a point-source in 2D that moves according to a trajectory $(X(t), Y(t))$ moving under (biased) Brownian motion for instance [see Eq. (1) or (9)], for which we have for $(x, y) \in \mathbb{R}^2$ and $t > 0$

$$-D\Delta c = \gamma(t)\delta(x - X(t), y - Y(t)). \tag{15}$$

Here $c$ denotes the concentration of the chemical, which diffuses with a diffusion coefficient $D$. Further, $\gamma$ denotes the strength of the point-source, which may change in time as a result of being present or not being present, and $\delta(.)$ denotes the Dirac Delta Function. The solution to this differential equation is given by

$$c(t, (x, y)) = -\frac{\gamma(t)}{2\pi D}\ln((x - X(t))^2 + (y - Y(t))^2), \tag{16}$$

in $\mathbb{R}^2$, which can be found in textbooks like for instance [27]. For the 3-D case, we report that the Green's Function is given by

$$c(t, (x, y, z)) = \frac{1}{4\pi D||\mathbf{x} - \mathbf{X}(t)||}, \tag{17}$$

In the case of multiple, say $n$, sources, with intensities $\gamma_j$ and positions $(X_j(t), Y_j(t))$, linearity of the diffusion equation allows us to use the superposition principle, to obtain

$$c(t, (x, y)) = -\sum_{j=1}^{n} \frac{\gamma_j(t)}{2\pi D}\ln(||\mathbf{x} - \mathbf{X}_j(t)||^2). \tag{18}$$

For a continuously distributed source-function $Q(t, (x, y))$ that is non-zero in $\Omega \subset \mathbb{R}^2$, we get the following convolution-based solution

$$c(t, (x, y)) = -\frac{1}{2\pi D}\int_{\Omega} Q(t, (\overline{x}, \overline{y}))\ln(||\mathbf{x} - \overline{\mathbf{x}}||^2)d\overline{\Omega}, \tag{19}$$

where the above integral is evaluated over $(\overline{x}, \overline{y})$. The 3D case can be treated analogously.

For the case of a transient diffusion field, we proceed analogously to the steady-state case with the application of delta-functions to deal with the point sources, then we arrive at

$$\frac{\partial c}{\partial t} - D\Delta c = \gamma(t)\delta(x - X(t), y - Y(t)), \quad \text{for } (x, y) \in \mathbb{R}^2, t > 0, \tag{20}$$

in which we assume that $(X(t), \mathbf{Y}(t))$ represents a certain trajectory. Initially, the concentration is assumed to be zero, and then the following solution for the 2-dimensional case, as a Green's Function, is derived according to the principles outlined in Evans [27]:

$$c(t,(x,y)) = \int_0^t \frac{\gamma(s)}{4\pi D(t-s)} \exp\Big(-\frac{||\mathbf{x}-\mathbf{X}(s)||^2}{4D(t-s)}\Big) ds, \tag{21}$$

for the two-dimensional case and

$$c(t,(x,y,z)) = \int_0^t \frac{\gamma(s)}{(4\pi D(t-s))^{3/2}} \exp\Big(-\frac{||\mathbf{x}-\mathbf{X}(s)||^2}{4D(t-s)}\Big) ds, \tag{22}$$

for the 3-D case, see also Eq. (5). Using this Green's Function, any solution with sources having a compact support, but non-zero measure can be constructed, or any initial condition, by the application of superposition arguments that result into a convolution. For completeness, we give the result for $n$ discrete point sources at the points $(X_j(t), Y_j(t))$ and strength $\gamma_j(t)$ for $j \in \{1, \ldots, n\}$:

$$c(t,(x,y)) = \sum_{j=1}^{n} \int_0^t \frac{\gamma_j(s)}{4\pi D(t-s)} \exp\Big(-\frac{||\mathbf{x}-\mathbf{X}_j(s)||^2}{4D(t-s)}\Big) ds, \tag{23}$$

as well as for a 'continuous' source that lives in $\Omega \subset \mathbb{R}^2$, we get the following solution by the use of convolution

$$c(t,(x,y)) = \int_0^t \int_\Omega \frac{Q(s,(\overline{x},\overline{y}))}{4\pi D(t-s)} \exp\Big(-\frac{||\mathbf{x}-\overline{\mathbf{x}}||^2}{4D(t-s)}\Big) d\overline{\Omega} ds. \tag{24}$$

The treatment in $\mathbb{R}^3$ is fully analogous.

Next we consider the dynamics of the points on the cell boundary. Inertia is neglected in the present formalism. The computational domain may be given by a flat two-dimensional substrate, where we consider projections of cells or by a three-dimensional domain where cells move through extracellular matrix or a gel-like medium. We divide the circumference of the cell into $N$ points. On each point, the cell detects a chemical signal and each point moves according to the concentration gradient that is constructed by a (sequence of) fundamental solutions. Further the direction of motion, as well as the velocity of the points are determined by the degree of deformation. To this extent, we use the following phenomenological law for the motion of the gridpoints on the cell boundary

$$\mathbf{v}_i = \beta \nabla c(t, \mathbf{x}_i) + \alpha(\mathbf{x}_c(t) + \hat{\mathbf{x}}_i - \mathbf{x}_i(t)), \text{ for } i \in \{1, \cdots, N\}, \tag{25}$$

where $\beta$ denotes a mobility parameter of the cell boundary. This parameter is a measure for the deformation rate of the cell and also represents a measure of the sensitivity of the cell boundary to the concentration gradient. This $\beta$-term models chemotaxis. Further, the $\alpha$-term models the 'desire' of the cell to attain its

equilibrium shape and size. The parameter $\alpha > 0$ is a measure of the stiffness of the cell. The position of the point $i$, which depends on time, is denoted by $\mathbf{x}_i(t)$. The velocity of the point is denoted by $\mathbf{v}_i$. Further, the position of the cell center is given by $\mathbf{x}_c(t)$ and the initial positions of the boundary nodes minus the initial position of the cell center are denoted by $\hat{\mathbf{x}}_i$. The above equation guarantees that the velocity is directed towards the largest increase of the concentration, and that its magnitude depends on the magnitude of the concentration gradient. Note that in the case of repulsion, for instance due to a poison, the sign of the $\beta$-term should be reversed.

The movement of the cell boundary makes the cell deform and change its position. Furthermore, the cell area or volume changes as well. Since the cell consists of both fluids and solid polymeric matter, the cell is classically modeled as a visco-elastic medium. This means that the volume of the cell is not necessarily conserved. It is possible to inhibit volumetric changes by enlarging the $\alpha$-parameter if the volume of the cell increasingly differs from the initial cell volume. The model is described in more detail in Vermolen and Gefen [17]. An example of a three-dimensional computation of the model is shown in Fig. 3. The input-data were the same as in Vermolen and Gefen [17], see Table 1.

In this figure it can be seen how a cell deforms and migrates to engulf the bacteria. Once the bacteria have been neutralized, the cell deforms back to its equilibrium shape. In [17], the model is extended to multiple cells where each cell secretes an agent that attracts the other cells. The model is based on the assumption that a cell registers the difference between the present concentration profile and the concentration profile from its own secretion. A repulsive force between gridnodes on different cells is introduced to prevent the cells from overlapping. The phenomenological relation of the repulsive force is inspired by the Lennard–Jones potential from electromagnetics. Since the medium through in which the cells deform is nonhomogeneous and anisotropic, a stochastic component is added to the equation via a Wiener process. This makes Eq. (26) stochastic:

$$d\mathbf{x}_i = \beta \nabla c(t, \mathbf{x}_i)dt + \alpha(\mathbf{x}_c(t) + \hat{\mathbf{x}}_\mathbf{i} - \mathbf{x}_i(t))dt + \sigma d\mathbf{W}(t), \text{ for } i \in \{1, \cdots, N\}, \quad (26)$$

where $\mathbf{W} = (W_x, W_y, W_z)$ is a vector with Wiener processes $W_x$, $W_y$ and $W_z$ and $\sigma$ is a measure for the uncertainty (standard deviation) induced by nonhomogeneities of the medium. The first two terms are deterministic and hence represent classical drift. Some computed results with a stochastic contribution can be found in Vermolen and Gefen [17]. In this manuscript we only show a deterministic run in Fig. 3. In Fig. 4, we plot the times of engulfing a bacterium versus the cell stiffness and mobility. It can be seen that an increase of cell stiffness and/or a decrease of cell mobility delay the engulfment of bacteria. This computation can be used to quantify the influence of cell stiffening and motility decrease due to certain diseases. This simulation models the effectiveness of the immune response as a function of the properties of the immunity cells like white blood cells.

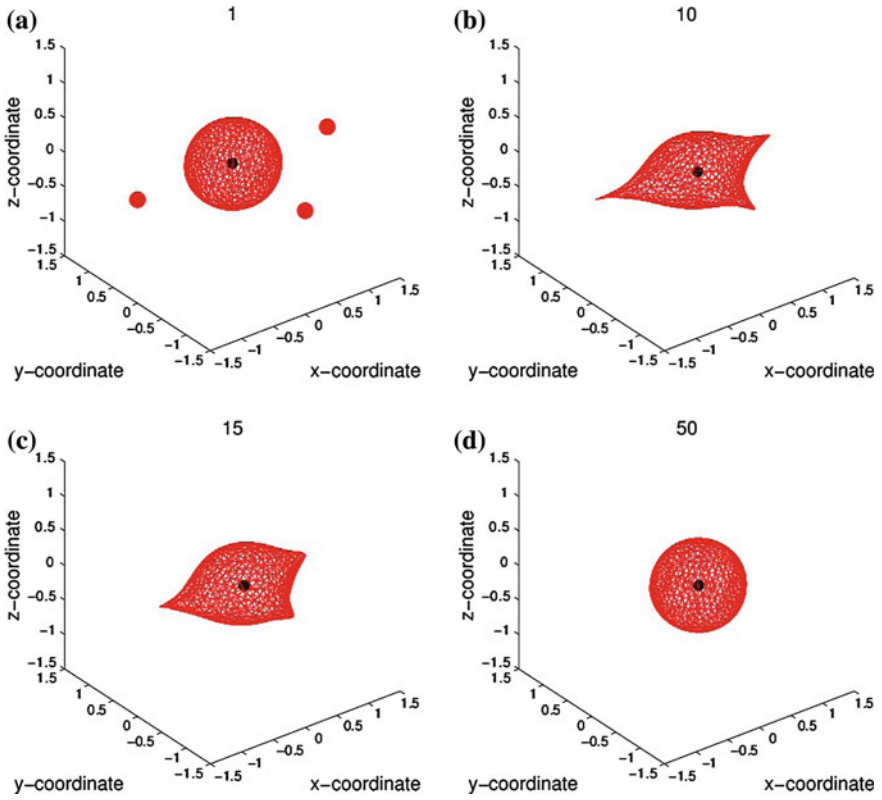


**Fig. 3** Snapshots at consecutive times of a cell engulfing bacteria

**Table 1** Values for the various parameters used

| Parameter | Value | Unit |
|---|---|---|
| $\beta$ | 5 | $mm^4/h/mol$ |
| $\gamma$ | 1 | $mol/mm^3/h$ |
| $\epsilon$ | 0.01 | $mm^6/h$ |
| $D$ | $\frac{1}{4\pi}$ | $mm^2/h$ |
| $\alpha$ | 1.5 | 1/h |

## 2.2 The Colony Scale

To make the present manuscript as self-contained as possible, we repeat some of the equations presented in Vermolen and Gefen [1]. Presently, we are also extending the model to simulate infected cell colonies. To this extent, we consider a flat substrate on which cells are allowed to move. The projection of the cells onto the substrate is assumed to be circular. Upon moving, each cell exerts a traction

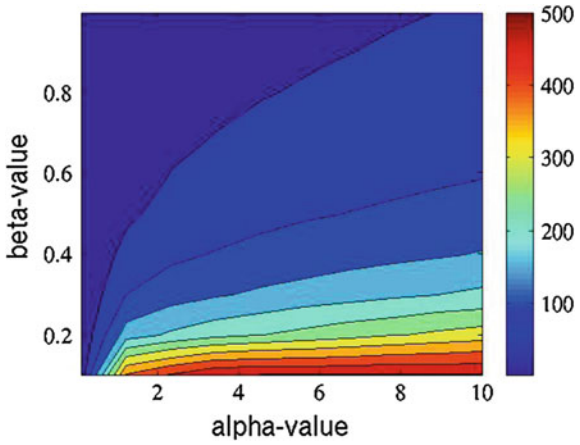


**Fig. 4** The engulfment time versus cell stiffness, $\alpha$, and cell mobility, $\beta$

force onto the substrate. This force generates a strain field around the cell that is sensed by the other cells if the strain energy density exceeds a certain threshold. In this way cells that are distant from each other sense each other's presence and hence these cells communicate with one-another, if they are not too far away from each other. This inter-cell communication over substrates through mechanical forces and sensing was experimentally observed by Byrne and Drasdo [2]. In this model, the deformation of the cells is not modeled, and cells are treated as circles with a constant radius $R$ and hence only the coordinate positions of the cell centres need to be computed and stored. In the present manuscript, we will disregard the randomness in the motion of the cells. In [1] a random contribution to cell movement is introduced via a uniform probability distribution. One could improve this formulation through a standard normal distribution so that the stochastic component is built up by a Wiener process. Besides movement of cells, we also incorporate the basic biological processes like cell division and death. Despite the fact that cell division and death can be predicted more-or-less if the entire history of a cell is known, these two fundamental processes are modeled as stochastic processes. The reason is that the history of the cells is not known and that the circumstances, although modeled as idealized, are not known well. In the model, we consider $n(t)$ cells. Due to cell division and death the integer $n$ depends on time. These cells are able to divide or die with respective probabilities $p$ and $q$ per unit of time. Further, the viable cells pull the substrate with a force $\hat{F}$, hence for cell $i$, we have

$$F_i = \begin{cases} \hat{F}, & \text{if the cell is viable} \\ 0, & \text{else} \end{cases} \tag{27}$$

The cells sense the strain energy density and the direction of the largest increase of this parameter, i.e. the gradient. Given a cell radius $R$ and a Young's Modulus of

the substrate $E_s$, the strain energy density as a result of cell $i$ pulling on the substrate is computed by

$$M_i^0 = \frac{1}{2}\sigma\epsilon = \frac{1}{2}E_s(\mathbf{r}_i)\epsilon^2 = \frac{F_i^2}{2E_s(\mathbf{r}_i)\pi^2 R^4}, \tag{28}$$

where the last step can be evaluated using some standard Hookean relations from mechanics, see [1]. In [1], we show by the use of finite-element simulations, that the strain energy density away from the cell can be approximated by

$$M_i(\mathbf{r}) = M_i^0 \exp\{-\lambda_i \tfrac{||\mathbf{r}-\mathbf{r}_i||}{R}\}, \qquad \text{for } \mathbf{r} \in \Omega, i \in \{1,\ldots,n\}, \tag{29}$$

where $\mathbf{r}_i$ represents the location of cell $i$, projected on $\Omega$, further $\lambda_i$ is a measure of how much the signal is attenuated, where we have

$$\lambda_i = \frac{E_s(\mathbf{r}_i)}{E_i}. \tag{30}$$

Here $E_i$ represents the Young's Modulus of the cell. Using the additivity-property of the strain energy density, the strain energy density for a superposition of cells is given by

$$M(\mathbf{r}) = \sum_{j=1}^{n} M_j(\mathbf{r}) = \sum_{j=1}^{n} M_j^0 \exp\{-\lambda_j \tfrac{||\mathbf{r}-\mathbf{r}_j||}{R}\}. \tag{31}$$

Let $\mathbf{r}_i(t)$ denote the position of the cell center $i$ at time $t$, then using this expression, the mechanical stimulus sensed by the $i$th cell is computed via

$$\begin{aligned} M(\mathbf{r}_i) &= \sum_{j=1}^{n} M_j(\mathbf{r}_i) = \sum_{j=1}^{n} M_j^0 \exp\{-\lambda_j \frac{||\mathbf{r}_i - \mathbf{r}_j||}{R}\} \\ &= M_i^0 + \sum_{j=1_{j\neq i}}^{n} M_j^0 \exp\{-\lambda_j \frac{||\mathbf{r}_i - \mathbf{r}_j||}{R}\}, \qquad \text{for all } i \in \{1,\ldots,n\}. \end{aligned} \tag{32}$$

Note that the cell's own contribution is also incorporated in this formula. Next, we repeat some of the formulas in Vermolen and Gefen [1] for the determination of the direction in which the cell is moving. The direction is determined by all the vectors connecting the other cells felt by the considered cell. The weight factors are given by the strength of the signal, in this case the strain energy density, experienced by the cell. This implies the following (deterministic) direction:

$$\mathbf{z}_i = \sum_{j=1_{j\neq i}}^{n} M_j(\mathbf{r}_i(t)) \frac{\mathbf{r}_j - \mathbf{r}_i}{||\mathbf{r}_j - \mathbf{r}_i||}, \text{ for all } i \in \{1,\ldots,n\}, \tag{33}$$

where a contributing term is mapped onto zero if $||\mathbf{r}_i - \mathbf{r}_j|| = 0$. The unit vector follows from the normalization:

$$\hat{\mathbf{z}}_i = \frac{\mathbf{z}_i}{||\mathbf{z}_i||}. \tag{34}$$

The velocity vector is constructed by the multiplication of this direction vector by the signal strength that is sensed by the considered cell to obtain:

$$\mathbf{r}_i'(t) = \alpha_i M(\mathbf{r}_i)\hat{\mathbf{z}}_i. \tag{35}$$

Here the cell velocity is modeled as instantaneous. In [18], we present a modification to incorporate the inertia effects into this formulation. The above equation can also be enriched with a stochastic contribution as is done in Vermolen and Gefen [1] using a uniform distribution or using Brownian Motion as in Eq. (9). Further, $\alpha_i$ is a velocity parameter with a dimension $\left[\frac{m^2 s}{kg}\right] = \left[\frac{m^3}{Ns}\right]$, determined by

$$\alpha_i = \left(\frac{F_i}{\hat{F}}\right)^2 \beta_i \frac{R^3}{f}. \tag{36}$$

Note that $\hat{F}$ is a property of the specific phenotype of the cell. The coefficient $\beta_i$, with unit $s^{-1}$, accounts for the mobility of the viable cell over the substrate surface. In [18], we incorporate the concentration of an infectious agent that typically results from bacteria. The cell-substrate friction effectively represents the averaged contribution of focal adhesions along the entire base of the cell without considering each localized connections of integrins. In [1], it is shown that $\alpha_i$ is determined by

$$\alpha_i = \frac{\beta_i R^3}{\mu \hat{F}^2} F_i, \tag{37}$$

where $\mu$ ($=0.2$ following [28]) denotes the cell friction coefficient. In [18], inertia is taken into account. Since this effect is known to be small, this effect is omitted in the present manuscript.

The cells will push each other away if they are too close together. This will give rise to repelling contact forces once these cells impinge elastically. The contact forces are due to the linear deformation of the cell bodies. In the present manuscript, the principles outlined in Gefen [28] are used. In [1], the derivation of the *invagination force* based on the work in Gefen [28] is given. In this manuscript, the final result for the strain energy density is given, which reads as

$$M^{ij} = \frac{6}{15} \frac{\sqrt{R^*} E^* h^{\frac{5}{2}}}{\pi R^3}, \tag{38}$$

where $h = \max(2R - ||\mathbf{r}_{ij}||, 0)$ is the indentation of cell $i$ into cell $j$ and vice versa. The final result for the total strain energy density function becomes

$$\hat{M}_i(\mathbf{r}) = M_i(\mathbf{r}) - M^{ij}, \tag{39}$$

**Table 2** Input data

| Quantity name | Symbol | Value | Unit |
|---|---|---|---|
| Substrate elasticity | $E_s$ | 5 | kPa |
| Cell elasticity | $E_c$ | 0.5 | kPa |
| Cell radius | $R$ | 4 | μm |
| Cell traction force | $\hat{F}$ | 1 | μN |
| Cell death probability | $p$ | 0.001 | – |
| Cell division probability | $q$ | 0.005 | – |
| Probability of velocity perturbation | $p_{mp}$ | 0 | – |
| Cell mobility coefficient | $\beta_i$ | $0.167 \cdot 10^{-3}$ | $s^{-1}$ |
| Initial relaxation parameter | $\kappa$ | 1000 | $s^{-1}$ |
| Friction coefficient | $\mu$ | 0.2 | – |

where $\hat{M}_i$ and $M^{ij}$ respectively denote the total strain energy density and the contribution to the strain energy density from the elastic interaction between neighboring cells. This quantity should be regarded as some energy relative to a certain energy level or as a potential in order to allow it to have negative values. For more details, we refer to [1]. The data that we use here can be found in Table 2.

We show some snapshots of a cell-colony simulation for 'wound healing' in Fig. 5. The red dots denote the cells that are moving towards each other as a result of mechanical pulling and their mechanical sensing. The snapshots at consecutive times show how the 'wound' closes. Further, we show the 'wound area' versus time in Fig. 6. It can be seen that first the 'wound' expands a bit and subsequently the 'wound' contracts. The curve shows a bit of noise that originates mainly from the randomness in cell division and cell death. The overall curve looks like a sigmoid relation. This is confirmed by in-vitro experiments on cell colonies. If one likes to model angiogenesis and its relation to wound healing, one could use a cellular automata model for instance and combine this model with the presently described model.

## *2.3 The Tissue Scale*

In order to be able to perform simulations over larger volumes and areas of tissues, individual cells are no longer tracked. Instead, cell densities are considered. In other words, the number of cells per unit volume or area is considered. This approach gives a system of partial differential equations (PDEs) where densities of several cell types are considered. In [29], among many other studies, a PDE-model for cutaneous wound healing is considered in terms of tracking the densities of fibroblasts, endothelial cells (to model angiogenesis), and keratinocytes are considered. The right-hand side in the above PDE contains a logistic growth term to account for an increase of cell density towards an equilibrium (i.e. the undamaged state). Furthermore, the levels of oxygen, VEGF, and extra-cellular matrix are

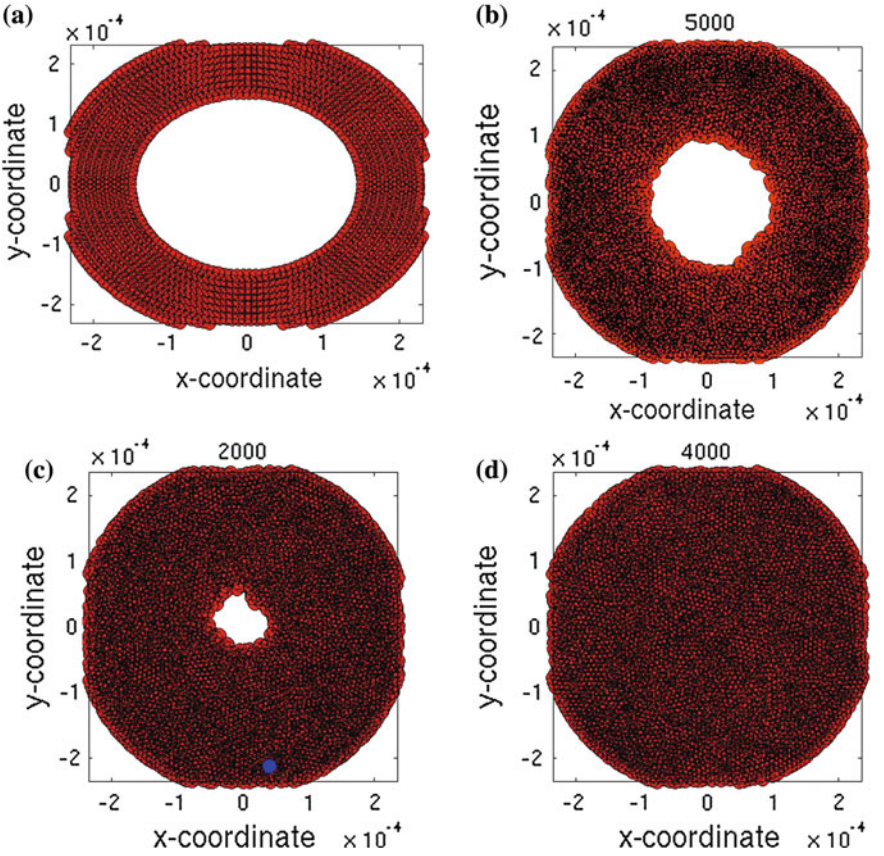


**Fig. 5** Four snapshots of a closing gap: **a** the initial state, **b** after 4 h, **c** after 15 h, and **d** after 32 h

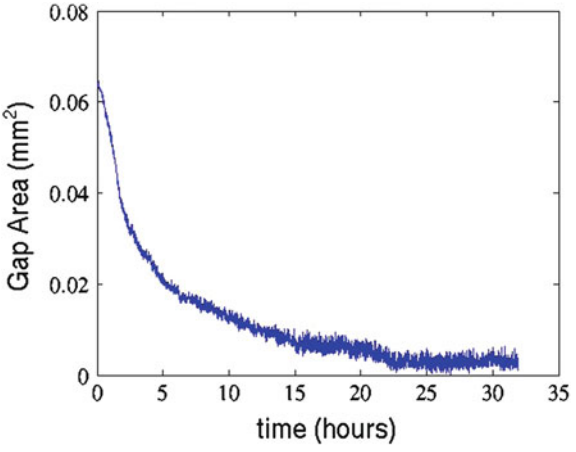


**Fig. 6** The gap area as a function of time

considered in the model. Next to these biological quantities, the local stress-strain pattern as a result of the contractile forces exerted by fibroblasts are dealt with by the solution of visco-elastic equations (Maxwell-model). This class of models is useful to model processes like angiogenesis, wound contraction and wound closure and this class has also be extended to model processes like tumor growth. An advantage of this model class is its applicability to in-vivo cases. Unfortunately, this class of models that contains a system of complicated nonlinear PDEs suffers from the incorporation of huge number of parameters which often are hard to measure. In this manuscript, we will not present a detailed model for wound healing, however, we will give a very simplified flavor of this model class by the consideration of a single partial differential equation that can be used to model wound closure in an in-vitro setting. To this extent, we consider the relatively simple Fisher–Kolmogorov equation, which reads as

$$\frac{\partial u}{\partial t} - D\Delta u = ku(1 - \frac{u}{u_0}), \qquad t > 0, (x, y, z) \in \Omega, \tag{40}$$

subject to some initial condition, that reads as

$$u(0, (x, y, z)) = u_0(x, y, z) = \begin{cases} u_0, & (x, y, z) \notin \Omega_w, \\ 0, & (x, y, z) \in \Omega \setminus \Omega_w. \end{cases} \tag{41}$$

Here $u$ denotes the cell density, $u_0$ denotes the undamaged equilibrium cell density and $\Omega_w$ denotes the area of the initial wound. Furthermore, in the PDE cell motion is determined through random walk only and the right-hand side models growth of the cell population towards an equilibrium. A snapshot at 12.5 h of the cell density (number of cells per unit volume or area, normalized to unity) is shown in Fig. 7. We used an initial circular 'wound' of radius 1 mm, $D = 10^{-4}\,\mathrm{mm}^2/\mathrm{h}$, and $k = 0.7\,\mathrm{h}^{-1}$. If one also encounters chemotaxis, then the cells move according to the concentration gradient of a generic chemical. Each cell moves according to the aforementioned concentration gradient, hence in the case of $u$ cells per unit area or volume, the amount and direction of cell movement are determined by the concentration gradient of the chemical multiplied by the cell density $u$, which gives

$$\frac{\partial u}{\partial t} - D\Delta u + \nabla \cdot (u\beta\nabla c) = ku(1 - \frac{u}{u_0}), \qquad t > 0, (x, y, z) \in \Omega, \tag{42}$$

where $\beta$ and $c$, respectively, denote the sensitivity and motility of the cells as a result of chemotaxis, and the concentration of the chemical that gives rise to chemotaxis. Here also a profile of the chemoattractant needs to be determined, which already increases the parameter space considerably. Note that the above equations corresponds to a drift term that is given by $\beta\nabla c$ in the stochastic counterpart. This equation models mobility of cells towards the concentration gradient of $c$, whereas reversing the sign would model mobility of cells away from the concentration gradient. In the case of a bounded domain of computation, then

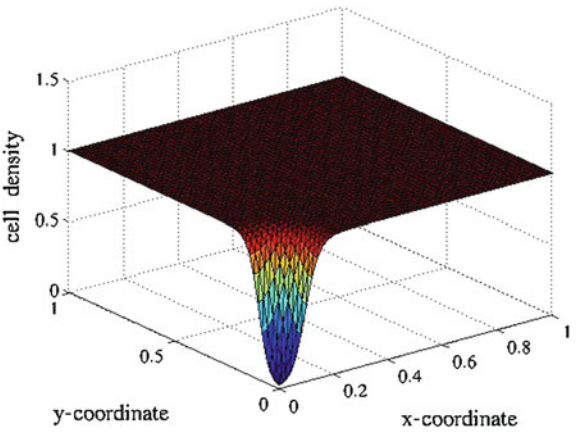


**Fig. 7** A snapshot of the solution to the Fisher–Kolmogorov equation as an elementary model for wound healing

one needs to formulate a boundary condition, such as setting the cell density equal to the equilibrium undamaged cell density or by imposing a no-flux condition. The Fisher–Kolmogorov equation admits traveling wave solutions, see [30] for instance. Furthermore, in a bounded domain, one often solves this PDE by the use of discretization techniques, such as the finite-element method. The wound boundary, which moves in time, is classically tracked as a level-curve of the cell density. The choice of the value for the level-curve is somewhat arbitrary, however, it gives a good qualitative picture of the kinetics of wound healing predicted by this simplified version of the PDE-continuum based models. Using the principles that were outlined Sect. 2.1.1, one can also regard the cell density as a measure for the likelihood to encounter a cell at a certain position and time. If cells are considered as point masses, then the principles outlined in Sect. 2.1.1 are helpful. However, if cells get compressed, then one should incorporate the cell volumes or areas. In the case of 'supersaturated' cell colonies, the cells are compressed and thereby their sizes are small. On the contrary, the 'subsaturated' cell colonies, in general contain elongated cells and thereby the sizes are larger. In both cases the same portion of the computational domain can be considered and hence the likelihood to find a cell at a certain position and time could thereby be equal. Hence the probability measures nonlinearly with the cell density in case of relatively large cells which cannot be treated by the use of point sources. Therefore, it was argued by Vermolen et al. [21] that the likelihood proceeds nonlinearly and that the curve of the likelihood versus the cell density exhibits a concave-downward relationship. An alternative point of view is to use the solution $u$ to represent the quality of the tissue at a certain position, where $u = u_0$ represents the undamaged quality which could be equal to unity. The quality of the overall tissue could be quantified by

$$Q(\Omega) = \frac{\int_\Omega u d\Omega}{u_0 Area(\Omega)}. \tag{43}$$

In this way, the quality of the tissue can be evaluated over time within a certain region, which also gives a useful indication of how the wound heals. This can be applied to more complicated models based on the solution of PDEs. We note that the computational model is extremely simple, and we refer for more complicated mathematical models to Vermolen and Javierre [29].

## 3 The Relation Between the Scales Involved

The three model classes give insights in their own way in their own scales. The cell-level models tell us how the shape of the cell actually behaves during the process of migration, which plays a major role in wound closure, wound contraction, but also in processes like tumor growth, as well as in the immune system. The measure of how much a cell can deform depends on its stiffness. Diseases that impair the cell stiffness (by for instance making the cell stiffer), will influence how the cell deforms when it is moving. In the case of the immune system, more elastic cells need to migrate over an only smaller distance to engulf a bacterium or any other harmful agent, see Fig. 4. This means that the bacteria or agents are neutralized within less time, and that less energy is consumed if the cell is flexible. In future studies, we will analyze the energy consumption of the immune system. Thereby, it can be concluded that the cell stiffness influences the efficiency of the immune system, next to the known parameters like the blood vessel stiffness and the number of white blood cells in the sense that if the cells are stiffer for some reason then the immunity response becomes less efficient. This holds for the immune system but also for the cells (for instance fibroblasts) that converge during processes like wound healing. The reason is that if cells converge to each other and if cells are relatively stiff, then it will take more time until cells are in physical contact. During the early stages of wound healing, flexible cells will be elongated as they move towards each other. Hence at the earliest stages at which the wound is closed, the cells are elongated if they are flexible. In the course of time as more cells have appeared due to cell division, the cells will get their cobble-stone shape. An example of a micrograph with different cell shapes in a cell colony is shown in Fig. 8.

If the cells are very stiff, then wound closure will be retarded since the cells are not able to elongate and hence the state of wound closure with elongated cells, which is the first stage of the wound being fully or partly closed, does not exist. Hence, the cell deformation model is very helpful in predicting the macroscopic closure rate of the wound. This issue will be investigated quantitatively in future.

The results from the cell colony model describe the nature how large numbers of cells converge, divide and die during processes like wound healing or tumor growth. In these models cell velocities, as well as cell division and death rates are used. These quantities are relatively easy to measure and thereby a good estimate of the wound healing kinetics can be obtained. Furthermore, the biological nature of wound healing is evaluated by monitoring the shape of the wound edge, and a

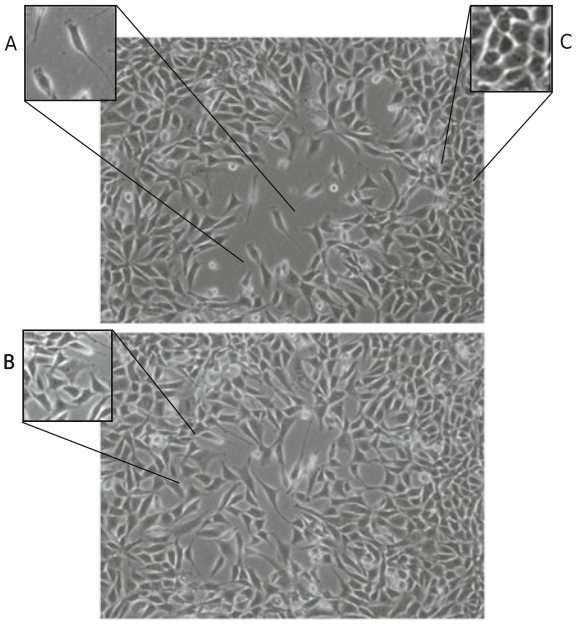


**Fig. 8** Two time-sequence micrographs, taken 4 h apart, which demonstrate shape changes in NIH3T3 fibroblasts which cover a local damage site: **A** oval elongated shape of migrating cells. **B** Multi-polar cell shapes when cells are resting and well-spread at a sub-confluent density; note the 4-poles cell in the center of the magnified frame. **C** Polygonal cell shapes in dense confluent sites. The scale-bar represents 100 μm

close link to in-vitro experiments with one-layer cell colonies can be established easily. Note that in the cell deformation model we considered a chemical signal driving cell edge mobility. Without any complication, it is mentioned that the mathematical nature of this signal is very generic and hence that this signal can also represented by a strain energy density as in the cell colony model. This generic nature of course also applies for the cell colony model where we could use a chemical signal using the same mathematical principles. Both the cell-scale and colony-scale models can model processes like chemotaxis and tensotaxis.

The transfer of the information from the cell colony model and hence also from the cellular model, in a certain sense is done by considering the theory outlined in Sect. 2.1.1 in case of random walk with a well-defined drift component. It can be seen that the cell diffusivity is related to the average cell velocity. This, however, only holds for the treatment of cells as so-called point sources that move independently. Incorporating the cell areas or volumes will make the treatment more challenging. However, if the cells or bacteria are sufficiently small compared to the mean distance they travel over a certain amount of time, then the approach in Sect. 2.1.1 is quite reasonable. The incorporation of chemotaxis, or analogously tensotaxis, the amount of biomass per unit area or volume that moves over a certain distance within a unit of time is proportional to the number of cells per unit volume or area, that is the cell density, times the concentration gradient scaled by a factor of proportionality. This is how the classical linear version of the Keller–Segell model for chemotaxis results. The continuum-based scale allows the use of larger tissue areas and hence allows to consider realistic in-vivo wound sizes. The transfer from colony models to PDE models, also strongly depends on the modes

that are incorporated in the modeling. If migration of cells is not only random, nor determined by any chemical signals, then, the tensotaxis could be modeled, which results into a completely different model where the diffusivity-tensor depends on the local strains. We note that the total local strain-tensor at any point within the domain of computation is determined by taking summing over the contributions of all individual cells. In a PDE-setting, one has to evaluate the cell density, which is the number of cells per unit of area or volume, and the forces that they exhibit. In our colony model, the strain energy density is evaluated as a result of adding the contributions of all individual cells that are present in the colony. To upscale this tensotaxis is by all means less trivial to carry out then upscaling processes like chemotaxis or random walk, and hence this is a challenge for future research. Though, it is tempting to upscale the models and many processes, though in some cases it is very difficult to incorporate all the information from the models. An example is the size of the cells in the colony models. The cell size certainly has an influence on the modeling outcomes in the sense that if large cells disappear then a relatively large gap arises. This enlargement of the cell radius makes the profile more prone to noise.

## 4 Modeling Several Processes in Wound Healing

The models that we considered here are very generic of nature and until here the presentation has mainly focused on wound closure or gap closure. Apart from gap closure, infections are very common to occur in clinical or real-world wounds. To this extent, we also plan to model bacterial infections, in which bacteria compete with the basis cells, such as fibroblasts or keratinocytes, on nutrients and oxygen, and thereby increase the tension of biotic lactates, which increase the acidity. The colony model has been extended with bacteria that move around and divide randomly. Bacterial motion is purely modeled as a Wiener process, by the use of equation (Sect. 2.1.1) with a certain division and death probability and release rate of biotic lactates. This chemical release is modeled by the use of Green's Fundamental solutions to the diffusion equation, and therewith in fact, the concentration of lactates as a result of a score of bacteria is determined using a superposition argument. A pilot study has been carried out in Vermolen and Gefen [18]. In this work, it is assumed that the cellular mobility decreases with increasing concentration of biotic lactates. A final conclusion of this work is that the decrease of motility causes gaps not to close anymore, hence the initial wound does no longer close entirely and that 'micro-gaps', which result from local cell death, and which would normally be occupied by newly appearing daughter cells from cell division, are no longer filled up due to decreased cellular motility. Hence the decrease of cellular motility leaves the gap open (for a long time) and can also be held responsible for the decrease of the quality of tissue. In principle white blood cells clear up contaminants and bacteria, and therefore we are working on a

colony-model that also clears up the bacteria by introducing white blood cells into the model.

We extended the simulations that we showed here for the three-dimensional cells that deform and migrate to the case of white blood cells (leukocytes) that leave a small blood vessel to head for an infection to neutralize the bacteria present. This modeling is currently done by the use of colony models and cell deformation models. Here a translation to the use of PDEs for continuum models is also to be made. We are also in the process of doing this and the results will appear in future papers. A final stage is the remodeling stage where the tissue remodels to transform from a scarred state into the fully undamaged state. To simulate this remodeling process, which is important in the context of hypertrophic scar formation as a result of burns, both the cellular and PDE-based models will be very useful since fibroblasts having several properties due to various chemico-mechanical environments will be taken into account.

Until now, we described the modeling of several biological processes: cell division, cell migration (due to random walk, tensotaxis or chemotaxis). Immobile processes like maturation towards cell division or cell differentiation can be modeled in cell colonies like stochastic processes. In fact, if the entire history path in terms of the chemical and mechanical environment is known then the time at which the cell differentiates or divides is determined. This advocates for a deterministic approach for cell division or differentiation processes. An example of such a model can be found in the age-structured model by de Vries et al. [31] for the computation of age-distributions in population dynamics or Prokharau et al. [32] for the modeling of cell differentiation with a maturation space variable (which corresponds to complete differentiation whenever this variable is one and to a fully undifferentiated state whenever the value zero holds). The latter model also contains biological processes like cell migration and cell division. This modeling class is based on solving an advection equation for the cell density per unit of maturation and can be extended to the incorporation of the physical space to model cell migration. In real-world situations, the entire history path of the cells is not exactly known or even hardly known. To this extent, the hypothesis of deterministic modeling is violated and one has to rely on stochastic processes. In the current paper we limited ourselves to modeling cell division as a purely random process. Probably it is more accurate to model cell differentiation by means of both a stochastic and deterministic component.

## 5 Conclusions

We presented a review of our ongoing work in simulation of wound healing on various scales. All scales give their own bits of information: The cell-based model for cell deformation can be used to analyze the shape changes a cell experiences under the influence of an attracting or repulsing chemical or under the influence of a local strain pattern. The cell-colony models can be used to look at the dynamics

of large number of cells upon using just a few, well accessible parameters as a function of the local chemical condition of the substrate or tissue. Further, the third scale is based on the continuum-hypothesis and is hence based on (systems of) PDEs. These PDEs can be solved using discretization techniques such as finite-element techniques or discontinuous Galerkin methods combined with limiters when the equations are chemotaxis-dominated (or mathematically speaking, predominantly hyperbolic). The paper describes the relations between the various scales involved in terms of stochastic and deterministic relations.

## References

1. Vermolen, F.J., Gefen, A.: A semi-stochastic cell-based formalism to model the dynamics of migration of cells in colonies. Biomech. Model. Mechanobiol. **11**(1–2), 183–195 (2012)
2. Byrne, H., Drasdo, D.: Individual-based and continuum models of growthing cell populations: a comparison. J. Math. Biol. **58**, 657–687 (2009)
3. Sherratt, J.A., Murray, J.D.: Mathematical analysis of a basic model for epidermal wound healing. J. Math. Biol. **29**, 389–404 (1991)
4. Filion, J., Popel, A.P.: A reaction diffusion model of basic fibroblast growth factor interactions with cell surface receptors. Ann. Biomed.Eng. **32**(5), 645–663 (2004)
5. Maggelakis, S.A.: A mathematical model for tissue replacement during epidermal wound healing. Appl. Math. Modell. **27**(3), 189–196 (2003)
6. Gaffney, E.A., Pugh, K., Maini, P.K.: Investigating a simple model for cutaneous wound healing angiogenesis. J. Math. Biol. **45**(4), 337–374 (2002)
7. Murray, J.D.: Mathematical Biology II: Spatial Models and Biomedical Applications. Springer, New York (2004)
8. Maggelakis, S.A.: Modeling the role of angiogenesis in epidermal wound healing. Discr.Cont. Syst. **4**, 267–273 (2004)
9. Adam, J.A.: A simplified model of wound healing (with particular reference to the critical size defect). Math. Comput. Model. **30**, 23–32 (1999)
10. Vermolen, F.J., Adam, J.A.: A finite element model for epidermal wound healing. In:Computational Science, ICCS 2007. Springer, Heidelberg, pp. 70–77
11. Olsen, L., Sherratt, J.A., Maini, P.K.: A mechanochemical model for adult dermal wound closure and the permanence of the contracted tissue displacement role. J. Theor. Biol. **177**,113–128 (1995)
12. Alarcon, T., Byrne, H., Maini, P., Panovska, J.: Mathematical modeling of angiogenesis and vascular adaptation. In: Paton, R., McNamara, L. (eds.) Studies in Multidisciplinary, vol. 3, pp. 369–387 (2006)
13. Vermolen F.J.: A simplified finite element model for tissue regeneration with angiogenesis. ASCE J. Eng. Mech. 135(5), 450–460 (2009)
14. Javierre, E., Vermolen, F.J., Vuik, C, van der Zwaag, S.: A mathematical approach to epidermal wound closure: model Analysis and Computer Simulations. J. Math. Biol.doi: 10.1007/s00285-008-0242-7; http://www.springerlink.com/content/w4j6633345j7228k/fulltext.pdf (2008)
15. Tranquillo, R.T., Murray, J.D.: Continuum model of fibroblast-driven wound contraction inflammation-mediation. J. Theor. Biol. **158**(2), 135–172 (1992)
16. Pettet, G.J., Byrne, H.M., McElwain, D.L.S., Norbury, J.: A model of wound healing angiogenesis in soft tissue. Math. Biosci. **136**, 35–63 (1996)

17. Vermolen, F.J., Gefen, A.: A phenomenological model for chemico-mechanically induced cell shape changes during migration and cell–cell contacts. Biomech. Model. Mechanobiol. (2012, in press)
18. Vermolen, F.J., Gefen, A.: A semi-stochastic cell-based model for in-vitro infected 'wound healing through motility reduction. J. Theor. Biol. (Submitted, 2012), doi:10.1016/j.jtbi.2012.11.007
19. Groh, A., Louis, A.K.: Stochastic modeling of biased cell migration and collagen matrix modification. J. Math. Biol. **61**, 617–647 (2010)
20. CJones, G.W., Chapman, S.J.: Modeling growth in biological materials. SIAM Rev. **54**(1), 52–118 (2012)
21. Vermolen, F.J., Gefen, A., Dunlop, J.W.C.: In vitro 'wound' healing: experimentally based phenomenological modeling. Adv. Eng. Mater. **14**(3), B76–B88 (2012)
22. Vermolen, F.J., van Baaren, E., Adam, J.A.: A simplified model for growth factor induced healing of circular wounds. Math. Comput. Model. **44**, 887–898 (2006)
23. Vermolen, F.J., Javierre, E.: On the construction of analytic solutions for a diffusion-reaction equation with a discontinuous switch mechanism. J. Comput. Appl. Math. doi:10.1016/j.cam.2009.05.022 (2009)
24. Steele, J.M.: Stochastic Calculus and Financial Applications. Springer, New York (2001)
25. Kim, Y.-Ch.: Diffusivity of bacteria. Korean J. Chem. Eng. **13**(3), 282–287 (1996)
26. Neilson, M.P., MacKenzie, J.A., Webb, S.D., Insall, R.H.: Modeling cell movement and chemotaxis using pseudopod-based feedback. SIAM J. Sci. Comput. **33**(3), 1035–1057 (2011)
27. Evans, L.C.: Partial Differential Equations, Graduate Studies in Mathematics, vol 19, 2nd edn. Americal Mathematical Society, Providence **49**, 22–25 (1998).
28. Gefen, A.: Effects of virus size and cell stiffness on forces, work and pressures driving membrane invagination in a receptor-mediated endocytosis. J. Biomech. Eng. (ASME) **132**(8), 4501–4505 (2010).
29. Vermolen, F.J., Javierre, E.: A finite-element model for healing of cutaneous wounds combining contraction, angiogenesis and closure. J. Math. Biol. doi:10.1007/s00285-011-0487-4
30. Sachdev, P.L.: Nonlinear Diffusive Waves. Cambridge University Press, Cambridge (1987)
31. de Vries, G., Hillen, Th., Lewis, M., Müller, J., Schönfisch, B.: A Course in Mathematical Biology: Quantitative Modeling with Mathematical and Computational Methods. SIAM, Philadelphia (2006)
32. Prokharau, P.A., Vermolen, F.J., Garcia-Aznar, J.M.: Model for direct bone apposition on pre- existing surfaces during peri-implant osseointegration. J. Theor. Biol. **304**, 131–142 (2012)